ChemPhotoChem

Chemistry Europe
European Chemical Societies Publishing
ChemPhotoChem

RESEARCH ARTICLE OPEN ACCESS

Cannabinoid-Inspired Fluorescent Boroisoquinolines for CB_1 Receptor Imaging

Dénes Szepesi Kovács[1,2] | Csilla Nierner[1,3] | Bettina Szepesi Kovács[1] | Attila Lehotzky[4] | Edina Szűcs[1] | András Dávid Tóth[4,5] | Dóra Judit Kiss[1,2] | László Hunyady[4,6] | György M. Keserű[1,2,3] | Péter Ábrányi-Balogh[1,2,3]

[1]Medicinal Chemistry Research Group, HUN-REN Research Centre for Natural Sciences, Budapest, Hungary | [2]National Laboratory for Drug Research and Development, Budapest, Hungary | [3]Department of Organic Chemistry and Technology, Budapest University of Technology and Economics, Budapest, Hungary | [4]Institute of Molecular Life Sciences, Centre of Excellence of the Hungarian Academy of Sciences, HUN-REN Research Centre for Natural Sciences, Budapest, Hungary | [5]Department of Internal Medicine and Haematology, Semmelweis University, Budapest, Hungary | [6]Department of Physiology, Faculty of Medicine, Semmelweis University, Budapest, Hungary

Correspondence: Péter Ábrányi-Balogh (abranyi-balogh.peter@ttk.hu)

Received: 30 January 2026 | **Revised:** 13 August 2026 | **Accepted:** 24 August 2026

Keywords: boroisoquinoline | CB_1 receptor | fluorescent imaging | fluorophore | organic difluoroboron complex

ABSTRACT

N,*N*- and *N*,*O*-bidentate organic difluoroboron fluorophores can be developed from natural and synthetic molecules. We report here the multistep synthesis and characterization of fluorescent boroisoquinolines as *N*,*O*-bidentate-BF_2-complexes, structurally similar to cannabinoids. These compounds were envisaged to be CB_1 ligands with intrinsic fluorescence that enables their use in receptor imaging without the need for an additional fluorophore. Binding and functional activity of the most promising boroisoquinoline was confirmed on CB_1 receptors. This compound labeled CB_1 receptors effectively in live cells allowing confocal imaging. These features nominate this compound as a new intrinsically fluorescent probe for CB_1 receptor.

1 | Introduction

The complexation of the BF_2 functional group with nitrogen and oxygen atoms leads to fluorophores; among them, BODIPYs (**1**) are the most highlighted representatives [1–3]. Recently, further N—B—N [4, 5] or N—B—O containing chemotypes were published having diverse structures and improved photophysical properties (Figure 1A). The *N*,*O*-bidentate difluoroboron complexes–also called NBO-complexes or boranyls [6]–comprise boron-containing heterocycles (**2**,**3**) [7], such as borobenzothiazoles (**4**) [8], NBO-coumarins (**5**) [9], boroquinolines [10, 11], multi- [12], and polyboranyls (**6**,**7**) [13] and their clickable derivatives (**3**) [14]. Boranyls were reported to have acceptable to good quantum yields and excellent Stokes shifts, emitting light usually in the 380–680 nm range depending on the substituents. These compounds have been used in a wide range of photofunctional applications such as bioimaging, photosensitizing, laser dyes, solar cells, organic light-emitting diodes, and electron-transport materials, as well [15]. Our group developed the boroisoquinolines (**8**) and borocarbolines (**9**) turning alkaloids into fluorescent dyes that found application in analytical and medicinal chemistry [16–18]. A similar approach was reported recently, transforming ageladine A to a bright pH-dependent BF_2-complex analog (**10**) [19]. Aiming to find further applications to boroisoquinolines, we noticed that their tricyclic scaffold is similar to that of THC (**11**) and analogous CB_1 agonists (AM11542 (**12**), L759633 (**13**), and JWH133 (**14**), Figure 1B) [20]. CB_1 is part of the endocannabinoid system regulating critical functions and linked to a range of pathological conditions such as obesity, pain, heart failure, or epilepsy [21, 22]. Despite the significant unmet medical need, understanding its pathophysiological role and developing modulators are still challenging [21, 22]. Fluorescent probes have already been developed against the CB_1 receptor using the conventional approach connecting a known ligand to a fluorescent dye with a suitable linker (**15–17**, Figure 1C) [23–26]. We imagined boroisoquinolines as intrinsically fluorescent probes without

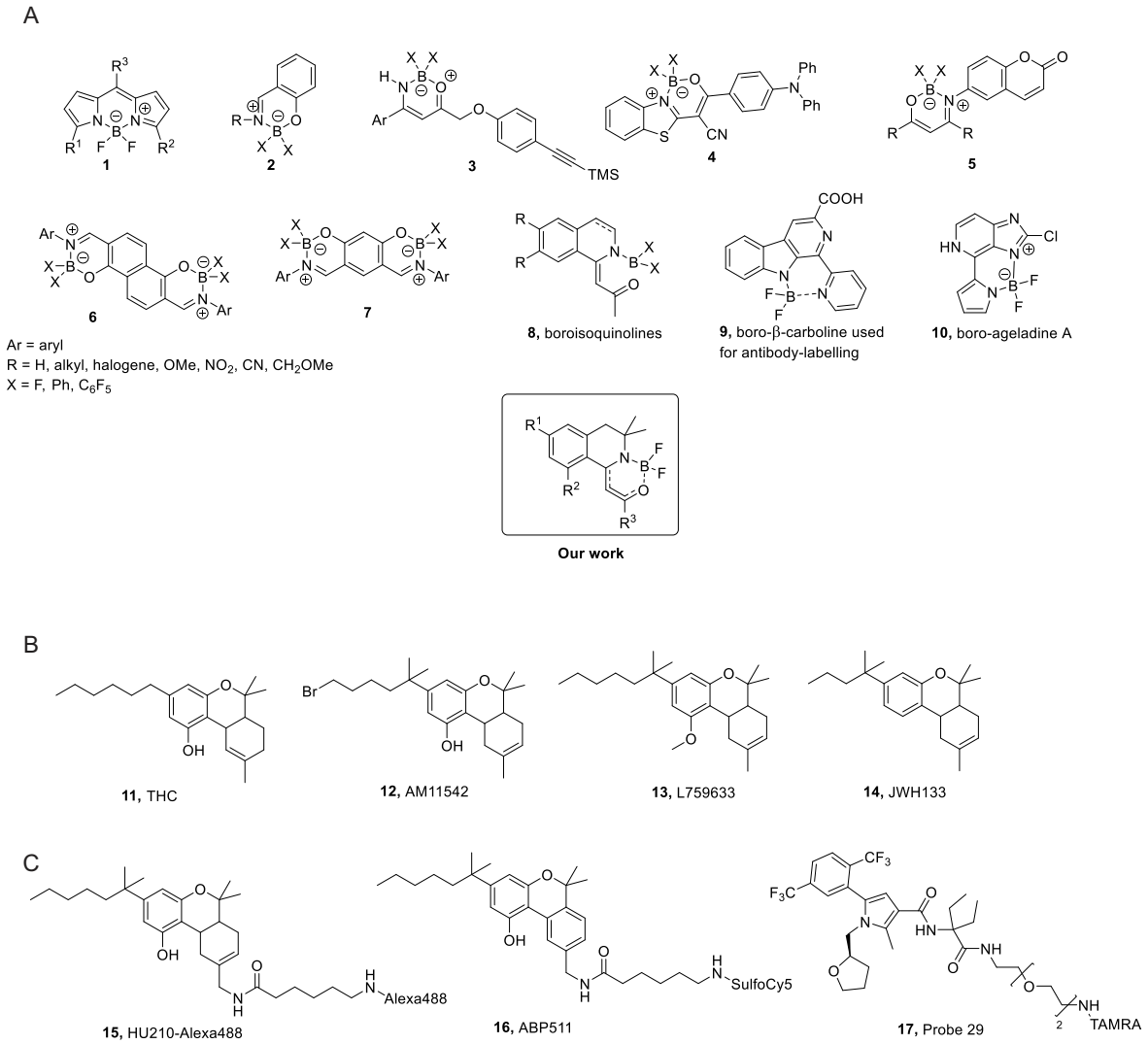

FIGURE 1 | (A) General structure of BODIPYs and selected examples of NBO-complexes. This work in frame. (B) THC and analogous CB_1 agonists. (C) Fluorescent probes for CB_1 receptor.

introducing further building blocks (linker and dye) that would prevent unwanted receptor interactions and preserve the binding mode of cannabinoids.

2 | Results and Discussion

Continuing our research on fluorescent dyes [27, 28], particularly BF_2 complexes, such as borocarbolines [16] and boroisoquinolines [17, 18], we synthesized a library of variously substituted boroisoquinolines to broaden the scope of this family, including derivatives inspired by structurally similar CB_1 receptor ligands [20].

For the synthesis of boroisoquinolines, phenylacetones (**18**) or phenylacetonitriles (**19**) were transformed into tertiary alcohols that contain the characteristic dimethyl group present in cannabinoids. Phenylacetones (**18a,b**) could be reacted by methylmagnesium iodide directly, resulting in the desired alcohols with good yields (**20a,b**, 70% and 71%, Scheme 1A), while phenylacetonitriles (**19a,b**) were first efficiently hydrolyzed to phenylacetic acids (**21a,b**, 78% and 86%) that were then transformed to the corresponding methyl esters (**22a,b**) (Scheme 1B). The esters (**22a,b**) were reacted with methylmagnesium iodide, leading to tertiary alcohols (**20c,d**) in good yield (66% and 71%, respectively). The tetrahydroisoquinoline ring was obtained in the Ritter reaction that was well tolerated in most cases (**23a–c,e–h**, 64%–93% yields), except **23d** (32%, Scheme 1C) [29]. The fluorine at the 6-position was substituted to pyrrolidine in an S_NAr reaction (**23i–k**), while the 6-bromo-derivative was coupled to *N*-hexyl-methylamine (**23n**). Both methoxy and amino substituents were installed as electron-donating moieties to improve fluorescence. In two cases, the 6-methoxy group was transformed to 6-hexyloxy by HBr-mediated demethylation followed by alkylation using hexyl bromide (**23l,m**). The methoxy and pyrrolidinyl derivatives served for the comparison of the oxygen- and nitrogen-based substituents, while **23l–n** contained a characteristic tail present in cannabinoids. Finally, the BF_2 group was installed using boron-trifluoride diethyletherate in the presence of DIPEA as a base with moderate to good yields (**24a–i**, 30%–87%, Scheme 1C).

Next, the absorption and emission spectra were recorded for **24a–i,** and we calculated Stokes shifts, molar absorption

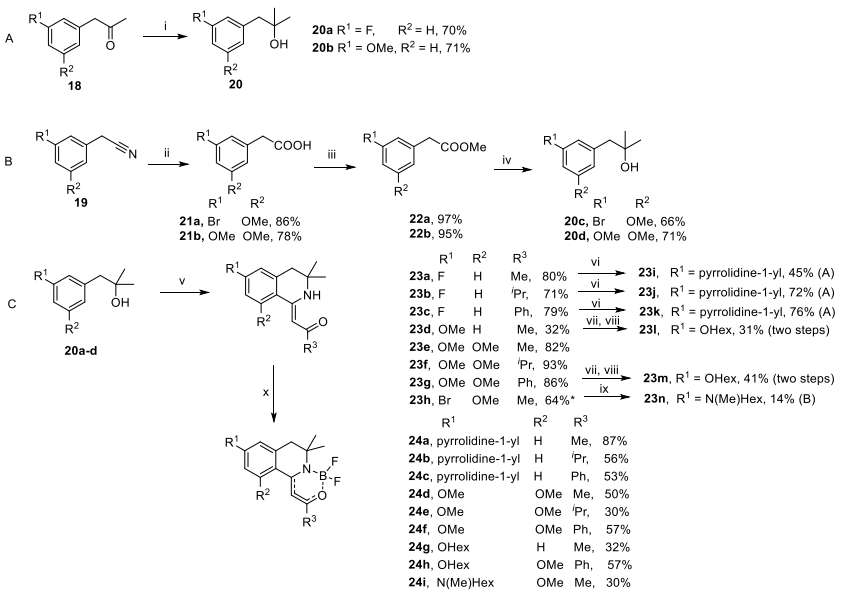

SCHEME 1 | Synthesis of boroisoquinolines. Reaction conditions: (A) i:MeMgI, diethyl-ether, RT, 0.5–2 h, Ar; (B) ii: cc. HCl, Δ, 1 h; iii: $SOCl_2$, MeOH, 0 °C then Δ, 30 min; iv: MeMgI, diethyl-ether, RT, 48 h; (C) v: 3-oxobutanenitrile or 4-methyl-3-oxopentanenitrile or 3-oxo-3-phenylpropanenitrile, cc H_2SO_4, 60 °C, toluene, 10–60 min; vi: pyrrolidine, 120 °C, dioxane, overnight; vii: HBr, AcOH, 120 °C, 48 h; viii: hexyl-bromide, K_2CO_3, DMSO, RT, overnight; ix: *N*-hexyl-methylamine, $Pd(OAc)_2$, KO^{t}Bu, JohnPhos, toluene, 80 °C, 48 h, Ar; x: $BF_3{\cdot}OEt_2$, DIPEA, DCM, RT, 0.5–4.5 h. *Reaction yielded two isomers with 64% and 54% yields (R^1 = Br, R^2 = OMe and R^1 = OMe, R^2 = Br).

TABLE 1 | Summary of photophysical characterization of boroisoquinolines.

#		R^1	R^2	R^3	ε, M^{-1} cm^{-1}	Φ_F, —	*B*, —	λ^{em}_{max}, nm	$\Delta\lambda$, nm
24a	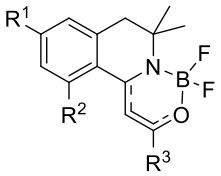	Pyrr	H	Me	27,196	0.97	26,380	448	67
24b		Pyrr	H	^{i}Pr	36,289	0.99	38,466	449	67
24c		Pyrr	H	Ph	41,895	0.39	16,339	534	128
24d		OMe	OMe	Me	24,358	0.0044	107	390	51
24e		OMe	OMe	Ph	22,195	0.0015	33	421	53
24f		OMe	OMe	^{i}Pr	26,788	0.0060	161	390	50
24g		OHex	H	Me	27,154	0.0057	155	389	64
24h		OHex	OMe	Ph	36,744	0.0022	81	418	71
24i		*N*(Me)Hex	OMe	Me	41,460	0.63	26,120	448	67

Note: Measurements were performed in acetonitrile.

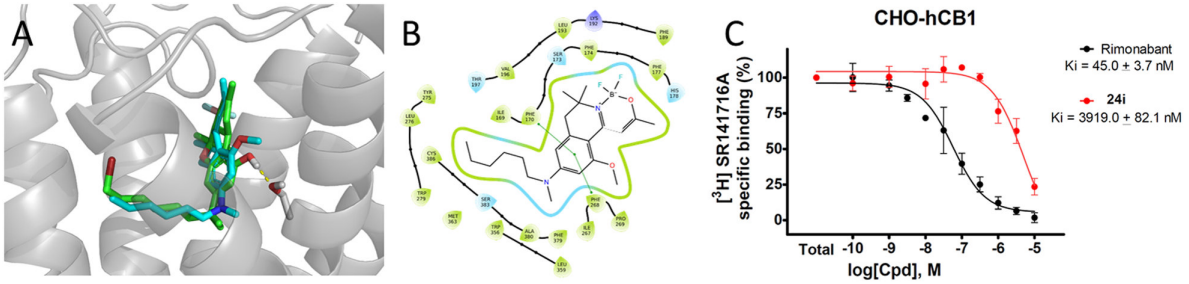

FIGURE 2 | (A) Overlapping binding mode of **24i** (cyan) and AM11542 (green). The hydrogen bonding interaction with Ser383$^{7.39}$ is indicated by yellow dashed line. (B) Binding interactions of **24i** in the CB_1 receptor (PDB 5XRA [30]). The aromatic stacking interactions are indicated by green lines. (C) Competitive binding of **24i** measured in radioligand displacement assay. Binding affinity of ligand was compared to SR141716A, a well-established CB_1 antagonist radioligand widely accepted for characterizing ligand binding at the orthosteric site in [^{3}H]SR141716A competition binding assays in membrane homogenates of CHO-hCB_1 cells. Values represent mean values ± S.E.M. for at least three experiments performed in duplicate. The IC_{50} values for the CB_1R according to the competition binding curves were converted into equilibrium inhibitory constant (K_i) values, using the Cheng–Prusoff equation [31].

coefficients (ε), quantum yields (Φ_F), and brightness (B) values (Table 1). We found that all compounds have fluorescence maxima between 389 and 534 nm, improved by the Ph substituent at R^3 (**24c,e,h**) or by the amino group at the R^1 (**24a–c,i**) position. Notably, for cannabinoids, the $R^3 = Me$ should be prioritized. Amino derivatives showed fluorescence at 448–449 nm or 534 nm. The Stokes shifts for all compounds were higher than 50 nm, and again, the presence of the phenyl (R^3) or amino (R^1) groups was highly beneficial (**24c,e,h** and **24a–c,i**, respectively). The molar absorption coefficients of the ethers (**24d–h**) were between 22,000–37,000 $M^{-1}cm^{-1}$, with low quantum yields (Φ_F 0.0015–0.0060), while ε for the amino

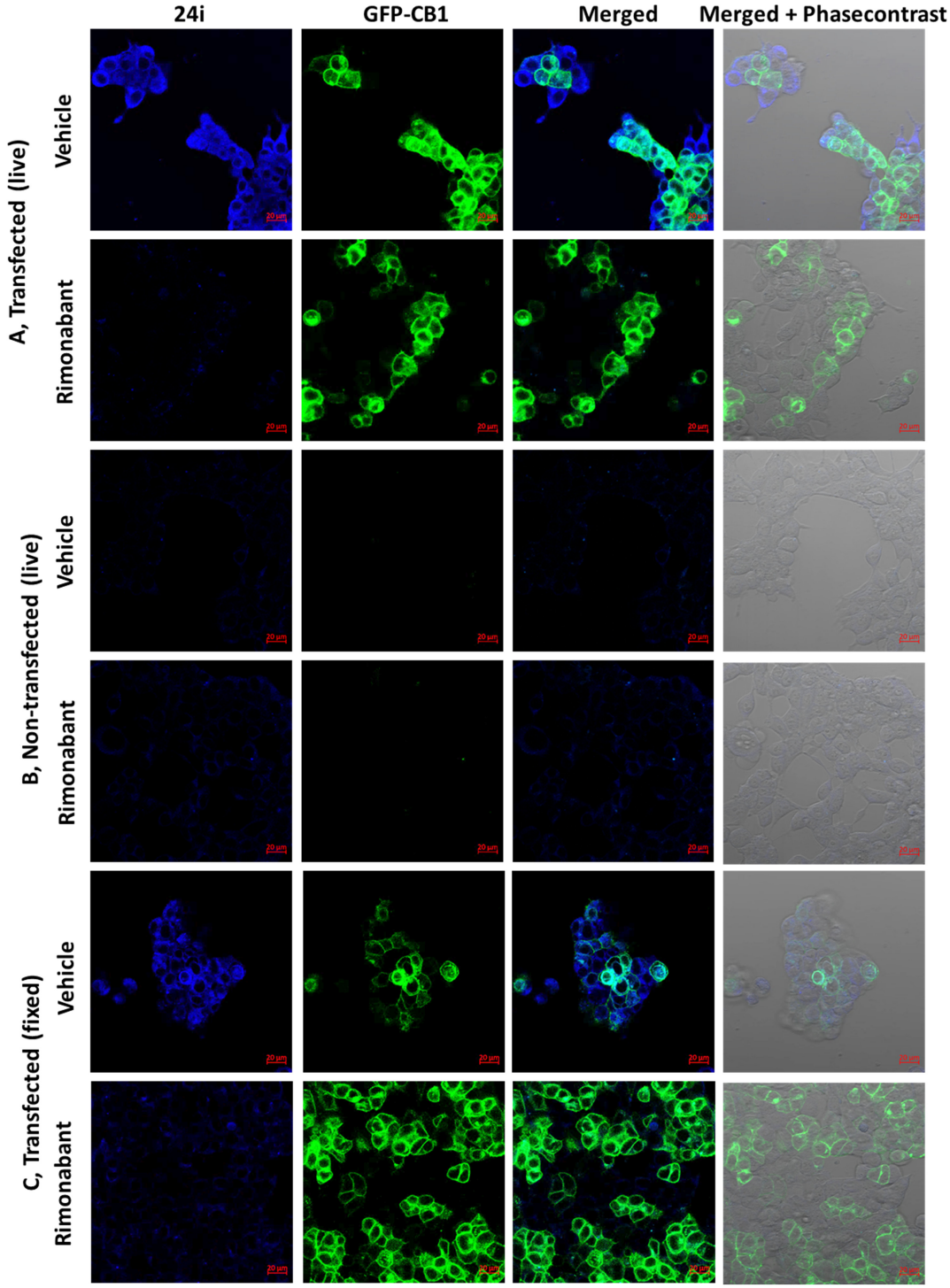

FIGURE 3 | Confocal microscopy images of **24i** (0.5 μM)-labeled HEK 293T cells. Blue color shows **24i** labeling, green color indicates fluorescence of GFP-CB_1. Cultures in some cases were grown in partially overlapping layers that may have led to signal contribution from adjacent layers at different focal planes. (A) Upper row: labeling of GFP-CB_1-transfected live HEK 293T cells. Lower row: labeling of GFP-CB_1-transfected live HEK 293T cells after rimonabant (5 μM) pre-treatment (5 min). (B) Upper row: labeling of non-transfected live HEK-293T cells. Lower row: labeling of non-transfected live HEK 293T cells after rimonabant (5 μM) pre-treatment. (C) **24i** labeling of GFP-CB_1-expressing HEK 293T cells after fixation. Live cells were pretreated with vehicle (upper row) or 5 μM rimonabant (lower row), incubated with **24i** for 2 min, washed, and fixed with PFA.

derivatives (**24a–c,i**) was higher (27,000–42,000 $M^{-1}cm^{-1}$), and their efficiency was significantly better (Φ_F 0.39–0.99).

Among these compounds, **24g** and **24i** were most similar to CB_1 ligands, having a long tail and a smaller R^3 substituent. Comparing them, compound **24i** showed the most promising photophysical properties. We measured its excitation and emission spectra in different solvents (Figure S1), and found slight hypsochromic and batochromic shifts, in apolar and polar solvents, respectively ($\lambda^{abs}_{max(PBS)}$ 388 nm > $\lambda^{abs}_{max(acetonitrile)}$ 381 nm > $\lambda^{abs}_{max(hexane)}$ 366 nm). The emission spectra follow a similar trend, resulting in higher Stokes shift in polar solvents ($\lambda^{em}_{max(PBS)}$ 459 nm, $\Delta\lambda_{PBS}$ 74 nm).

The binding mode of **24i** was predicted by docking to the orthosteric pocket of the CB_1 receptor. Due to the structural similarity of **24i** with AM11542, the CB_1 complex of this reference compound (PDB: 5XRA) [30] was used in our docking simulations. Docking calculations suggested that the stable binding mode of **24i** overlaps well with AM11542 (RMSD: 0.92 Å, Figure 2A). The heterocyclic cores show only a minor relative rotation, and the key hydrophobic interactions stabilizing binding—most notably the aromatic stacking interactions with $Phe170^{2.57}$ and $Phe268^{ECL2}$ (Figure 2B)—might be maintained. However, while AM11542 forms a hydrogen bond with $Ser383^{7.39}$ with its hydroxy group, this might be missing for **24i,** which has a methoxy group in the same position (Figure 2A). AM11542 is a low-nanomolar full agonist (K_i = 0.11 nM, EC_{50} = 3.4 nM, and E_{max} = 54.6%), while its methoxy analog L759633 (K_i = 1.0 μM, EC_{50} = 0.42 μM, and E_{max} = 21.5%) has lower potency and efficacy [20, 30, 32]. Consequently, the lack of this H-bond might explain the reduced affinity of **24i** compared to that of the reference (Figures 2C and S2).

The cannabinoid receptor binding affinity of **24i** was examined in [^{3}H]SR141716A homologous displacement experiments for CB_1R in CHO-hCB_1 cell line membrane homogenates. Boroisoquinoline **24i** displayed a micromolar affinity (K_i = 3.9 μM, Figure 2C). Functional activity was evaluated using a BRET-based G_{i1} protein activation assay [23]. The G_{i1} biosensor reports G-protein activation via dissociation of the G-protein subunits. In HEK 293T cells co-expressing the human CB_1 receptor, **24i** produced a partial, concentration-dependent sensor response (EC_{50} = 6.67 μM, E_{max} = 23.1%, Figures S2 and S3, Supplementary Discussion), whereas no effect was detected in cells transfected with the biosensor and an empty vector. These data support CB_1-dependent partial agonist activity of **24i** that corresponds to the functional activity of THC and is considered as a beneficial characteristic [33, 34].

Finally, GFP-CB_1-transfected live HEK 293T cells were treated with **24i** both in the presence and absence of rimonabant. After a short incubation time (2 min), confocal microscopy showed **24i** co-localization with the GFP-CB_1 signals (blue and green signals, respectively) when no rimonabant was present, but labeling was not observed in the presence of the antagonist (Figure 3A, upper and lower rows, respectively). Non-transfected cells showed no labeling by **24i** (Figure 3B). A clear specific signal was observed for approximately 5 min; however, after that, **24i** slowly accumulated at the cell membrane, and increased non-specific labeling was observed (data not shown). Therefore, the experiment was modified by removing the excess of **24i** after 2 min of labeling and fixing the cells. This protocol enabled **24i** labeling of GFP-CB_1 in the absence of rimonabant, whereas no labeling was seen after antagonist pretreatment (Figure 3C).

3 | Conclusions

Here, we report the synthesis and photophysical characterization of a set of boroisoquinolines that are structurally similar to cannabinoids. Among them, amino derivatives showed standout molar absorption coefficients and quantum yields with large Stokes shifts, emitting light above 440 nm. A selected derivative (**24i**) was subjected to biological evaluation and was identified as a low-micromolar partial agonist of the human CB_1 receptor. Selective imaging of CB_1 receptors was confirmed by confocal microscopy in live cells. The intrinsic fluorescence of our probe provides a unique opportunity for CB_1 imaging to keep receptor structure and pharmacology similar to that observed with natural cannabinoid ligands.

Author Contributions

D.S.K. synthesized and characterized compounds, performed microscopic imaging, analyzed the data, and prepared figures. C.N. and B.S.K. synthesized and characterized compounds. E.S. performed radioligand binding measurements. D.J.K. performed and analyzed molecular docking. A.D.T. designed and analyzed BRET measurements. A.L. performed BRET measurements. L.H. supervised BRET measurements. G.M.K. provided funding, supervised the project and wrote the manuscript. P.Á.-B. conceptualized and supervised the project, participated in synthesis and data analysis, prepared figures and wrote the manuscript.

Acknowledgments

The authors received funding from the National Research Development and Innovation Office of Hungary [PharmaLab (RRF-2.3.1-21-2022-00015) to G.M.K., L.H.; ADVANCED 151284 to (L.H.) and STARTING 152117 to D.J.K.] and the Hungarian Academy of Sciences (NAP2022-I-2/2022 NAP 3.0). P.Á.-B. was supported by the János Bolyai Research Scholarship of the Hungarian Academy of Sciences. We thank Dr. István Katona for kindly providing the GFP-CB_1 construct.

Funding

This study was supported by National Research Development and Innovation Office of Hungary (RRF-2.3.1-21-2022-00015, ADVANCED 151284 and STARTING 152117) and Magyar Tudományos Akadémia (NAP2022-I-2/2022 NAP 3.0 and János Bolyai Research Scholarship).

Conflicts of Interest

The authors declare no conflicts of interest.

Data Availability Statement

The data that support the findings of this study are available from the corresponding author upon reasonable request.

References

1. I. S. Yadav and R. Misra, "Design, Synthesis and Functionalization of BODIPY Dyes: Applications in Dye-Sensitized Solar Cells (DSSCs) and Photodynamic Therapy (PDT)," *Journal of Materials Chemistry C* 11 (2023): 8688–8723.

2. H. Ahmad, S. Muhammad, M. Mazhar, et al., "Unveiling Cellular Mysteries: Advances in BODIPY Dyes for Subcellular Imaging," *Coordination Chemistry Reviews* 526 (2025): 216383.

3. C. Yu, X. Fang, Q. Wu, et al., "A Family of BODIPY-Like Highly Fluorescent and Unsymmetrical Bis(BF_2) Pyrrolyl–Acylhydrazone Chromophores: BOAPY," *Organic Letters* 22, no. 12 (2020): 4588–4592.

4. C. Yu, X. Fang, H. Wang, et al., "A Family of Highly Fluorescent and Membrane-Permeable Bis(BF_2) Acyl-Pyridinylhydrazine Dyes With Strong Solid-State Emission and Large Stokes Shifts: The BOAPH Fluorophores," *The Journal of Organic Chemistry* 86 (2021): 11492–11501.

5. A. N. Bismillah and I. Aprahamian, "Fundamental Studies to Emerging Applications of Pyrrole-BF_2 (BOPHY) Fluorophores," *Chemical Society Reviews* 50 (2021): 5631–5649.

6. D. Frath, S. Azizi, G. Ulrich, P. Retailleau, and R. Ziessel, "Facile Synthesis of Highly Fluorescent Boranil Complexes," *Organic Letters* 13 (2011): 3414–3417.

7. K. Mitsudo, N. Maekawa, R. Magata, et al., "Synthesis of N, O-Bidentate Difluoroboron Complexes via Iodide-Promoted Demethylative Borylation," *Organic Letters* 27 (2025): 10636–10641.

8. L. Zhou, D. Xu, H. Gao, et al., "Effects of Cyano Groups on the Properties of Thiazole-Based β-Ketoiminate Boron Complexes: Aggregation-Induced Emission and Mechanofluorochromism," *RSC Advances* 6 (2016): 69560–69568.

9. H. Doušová, P. Šimůnek, N. Almonasy, and Z. Růžičková, "Synthesis, NMR, X-Ray and UV/Vis Characterization and Preliminary Luminescence Study of Some Boron β-Iminoenolates Having 6-Aminocoumarin Moiety," *Journal of Organometallic Chemistry* 802 (2016): 60–71.

10. S. M. Elbert, P. Wagner, T. Kanagasundaram, F. Rominger, and M. Mastalerz, "Boroquinol Complexes With Fused Extended Aromatic Backbones: Synthesis and Optical Properties," *Chemistry – A European Journal* 23 (2017): 935–945.

11. U. Balijapalli and S. K. Iyer, "Synthesis and Optical Properties of a Series of Green-Light-Emitting 2-(4-Phenylquinolin-2-yl)phenol–BF_2 Complexes (Boroquinols)," *European Journal of Organic Chemistry* 2015 (2015): 5089–5098.

12. M. Urban, K. Durka, P. Jankowski, J. Serwatowski, and S. Luliński, "Highly Fluorescent Red-Light Emitting Bis(boranils) Based on Naphthalene Backbone," *Journal of Organic Chemistry* 82 (2017): 8234–8241.

13. D. Frath, K. Benelhadj, M. Munch, J. Massue, and G. Ulrich, "Polyanils and Polyboranils: Synthesis, Optical Properties, and Aggregation-Induced Emission," *Journal of Organic Chemistry* 81 (2016): 9658–9668.

14. L. F. Minuti, M. G. Memeo, S. Crespi, and P. Quadrelli, "Fluorescent Probes From Stable Aromatic Nitrile Oxides," *European Journal of Organic Chemistry* 2016 (2016): 821–829.

15. R. J. Grams, W. L. Santos, I. R. Scorei, et al., "The Rise of Boron-Containing Compounds: Advancements in Synthesis, Medicinal Chemistry, and Emerging Pharmacology," *Chemical Reviews* 124 (2024): 2441–2511.

16. D. Szepesi Kovács, I. Hajdu, G. Mészáros, et al., "Synthesis and Characterization of New Fluorescent Boro-β-Carboline Dyes," *RSC Advances* 11 (2021): 12802–12807.

17. D. Sóvári, A. Kormos, O. Demeter, et al., "Synthesis and Fluorescent Properties of Boroisoquinolines, a New Family of Fluorophores," *RSC Advances* 8 (2018): 38598–38605.

18. D. Sóvári, G. M. Keseru, and P. Ábrányi-Balogh, "Application of Boroisoquinoline Fluorophores as Chemodosimeters for Fluoride Ion and Pd (0)," *Materials* 13 (2020): 199.

19. C. Tolle, M. Fresia, P. G. Jones, and T. Lindel, "Fluorescent BF_2 Complexes Inspired by Ageladine A," *ChemPhotoChem* 8 (2024): e202400065.

20. T. S. Thorsen, Y. Kulkarni, D. A. Sykes, et al., "Structural Basis of THC Analog Activity at the Cannabinoid 1 Receptor," *Nature Communications* 16 (2025): 486.

21. U. Grether, "Therapeutic Potential of Cannabinoid Receptors Type 1 and 2—Novel Insights for Enhancing the Chance of Clinical Success," *Pharmaceuticals* 18 (2025): 1324.

22. R. G. Pertwee, "The Pharmacology of Cannabinoid Receptors and Their Ligands: An Overview," *International Journal of Obesity* 30, no. 1 (2006): S13–S18.

23. S. Prokop, P. Ábrányi-Balogh, B. Barti, et al., "PharmacoSTORM Nanoscale Pharmacology Reveals Cariprazine Binding on Islands of Calleja Granule Cells," *Nature Communications* 12, no. 1 (2021): 1–19.

24. L. Mach, A. Omran, J. Bouma, et al., "Highly Selective Drug-Derived Fluorescent Probes for the Cannabinoid Receptor Type 1 (CB_1 R)," *Journal of Medicinal Chemistry* 67, no. 14 (2024): 11841–11867.

25. M. Martín-Fontecha, A. Angelina, B. Rückert, et al., "A Fluorescent Probe to Unravel Functional Features of Cannabinoid Receptor CB_1 in Human Blood and Tonsil Immune System Cells," *Bioconjugate Chemistry* 29, no. 2 (2018): 382–389.

26. L. Borrega-Roman, B. L. Hoare, M. Kosar, et al., "A Universal Cannabinoid CB_1 and CB_2 Receptor TR-FRET Kinetic Ligand-Binding Assay," *Frontiers in Pharmacology* 16 (2025): 1469986.

27. D. Szepesi Kovács, B. Chiovini, D. Müller, et al., "Synthesis and Application of Two-Photon Active Fluorescent Rhodol Dyes for Antibody Conjugation and In Vitro Cell Imaging," *ACS Omega* 8 (2023): 22836–22843.

28. D. Szepesi Kovács, B. Kontra, B. Chiovini, et al., "Effective Synthesis, Development and Application of a Highly Fluorescent Cyanine Dye for Antibody Conjugation and Microscopy Imaging," *Organic & Biomolecular Chemistry* 21 (2023): 8829–8836.

29. M. Ogawa, T. Yoshikazu, and A. Ohhata, "3,4 Dihydroisoquinoline Derivative Compounds and Drugs Containing These Compounds as the Active Ingredient," (2001), WO2002010135A1.

30. T. Hua, K. Vemuri, S. P. Nikas, et al., "Crystal Structures of Agonist-Bound Human Cannabinoid Receptor CB_1," *Nature* 646 (2025): 754–758.

31. C. Yung-Chi and W. H. Prusoff, "Relationship Between the Inhibition Constant (Ki) and the Concentration of Inhibitor which Causes 50% Inhibition (I50) of an Enzymatic Reaction," *Biochemical Pharmacology* 22 (1973): 3099–3108.

32. S. Brogi, F. Corelli, V. Di Marzo, et al., "Three-Dimensional Quantitative Structure–selectivity Relationships Analysis Guided Rational Design of a Highly Selective Ligand for the Cannabinoid Receptor 2," *European Journal of Medicinal Chemistry* 46 (2011): 547–555.

33. S. Dutta, B. Selvam, A. Das, and D. Shukla, "Mechanistic Origin of Partial Agonism of Tetrahydrocannabinol for Cannabinoid Receptors," *The Journal of Biological Chemistry* 298 (2022): 101764.

34. F. Shahbazi-Raz, D. Meister, A. Mohammadzadeh, and J. F. Trant, "How THC Works: Explaining Ligand Affinity for, and Partial Agonism of, Cannabinoid Receptor 1," *iScience* 28 (2025): 112706.

Supporting Information

Additional supporting information can be found online in the Supporting Information section. Supporting information is available free of charge. Supporting information contains: **Figure S1**. Excitation and emission spectra of **24i** in different solvents (in 5 μM concentration); **Figure S2**. G_{i1} biosensor activation. Concentration-response effects of **24i** were observed in human CB_1 (hCB_1) and G_{i1} BRET biosensor co-expressing HEK 293T cells (EC_{50} = 6.67 μM, E_{max} = 23.1%); CP55940 was applied as a reference agonist (EC_{50} = 4.56 nM). No effects of CB_1 ligands were detected in cells expressing empty vector (pcDNA3.1) plus the biosensor.; detailed experimental procedures; materials and methods; compound characterization; NMR spectra.